Tree Physiology, 2025, **45**, tpaf109
https://doi.org/10.1093/treephys/tpaf109
Research paper

Acclimation of mango (*Mangifera indica* cv. Calypso) to canopy light gradients—scaling from leaf to canopy

Alexander W. Cheesman[1,*], Kali B. Middleby[1], Ryan Orr[1,2], Liqi Han[3], Gerhard Rossouw[2] and Lucas A. Cernusak[1]

[1]College of Science & Engineering and Centre for Tropical Environmental and Sustainability Science, James Cook University, McGregor Road, Cairns, QLD 4878, Australia
[2]Queensland Department of Primary Industries, 28 Peters Street, Mareeba, QLD 4880, Australia
[3]The Queensland Alliance for Agriculture and Food Innovation, 306 Carmody Road, The University of Queensland, Brisbane, QLD 4072, Australia

*Corresponding author (alexander.cheesman@gmail.com)

Handling Editor: Sari Palmroth

Mango (*Mangifera indica* L.), a leading tropical fruit crop, is a prime candidate for intensification through modern orchard-management techniques, including canopy manipulation to improve light interception. This study investigated how leaf-level acclimation to light gradients within the canopy of a high-yield, dwarfing mango cultivar (Calypso™) could be used to examine integrated canopy-scale responses. We quantified foliar morphological, biochemical and physiological traits across a range of canopy positions using this information to model canopy-scale productivity within digital-twin representations of mango under both conventional (i.e., open-vase) and espalier-trellis training canopy systems. Key findings demonstrated that leaves exposed to higher light exhibited increased leaf mass per unit area, nitrogen content and photosynthetic capacity (A_{sat}), but decreased chlorophyll-to-nitrogen ratios and photochemical reflectance indices, reflecting trade-offs between light capture and photoprotection. Phenolic content increased under high irradiance, indicating investment in photoprotective compounds at the expense of net carbon gain. Modelled leaf-level productivity increased with light availability, following a Michaelis–Menten saturating response, with diminishing returns under high light. Digital modelling of canopy light interception revealed that espalier-trellis training enhanced light distribution efficiency per unit leaf area but resulted in a 6.5% reduction in total canopy productivity due to a smaller total canopy leaf area. However, when normalized by total canopy leaf area, the espalier-trellis system showed a 3.6% productivity advantage over conventional canopies at the time of year modelled. These results highlight the role of canopy structure and light-use efficiency in determining orchard productivity. Integrating spatially explicit mechanistic models with LiDAR-derived canopy data offers a promising pathway for designing high-density, resource-efficient mango orchards. Future work should expand modelling to account for dynamic canopy shape throughout the growing season and evaluate the interaction of modified canopy structures with environmental stressors, particularly under climate variability.

Graphical Abstract

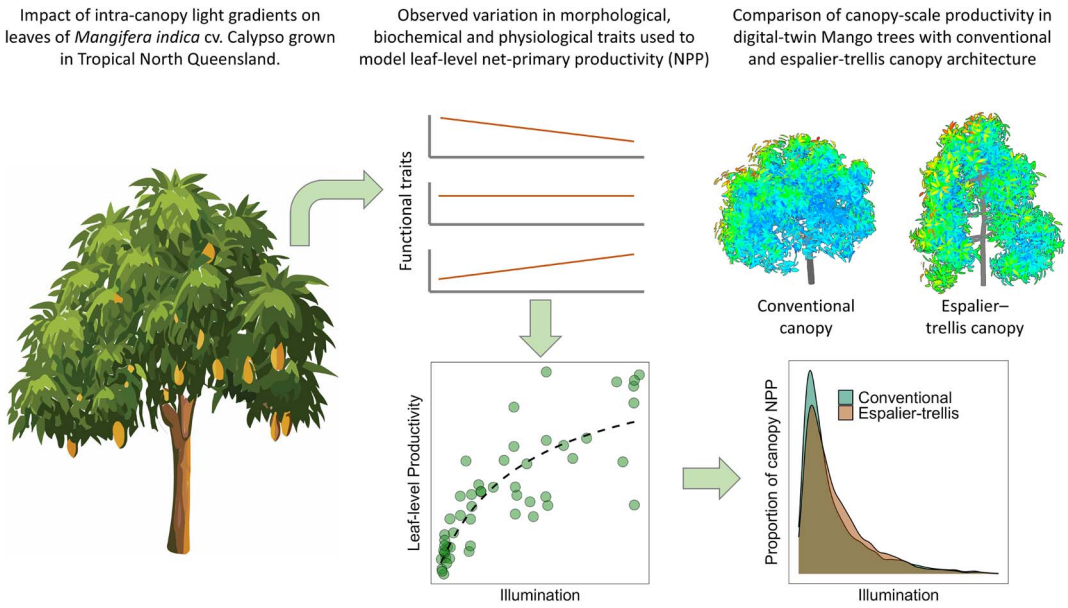

Keywords: canopy manipulation, digital twin, LiDAR, modelling, orchard systems, tropical agriculture.

Received: January 20, 2025. **Accepted:** August 29, 2025

Introduction

Globally, all food production systems must become more productive and resource-efficient to meet the needs of a growing population, and this is particularly the case in the tropics where population growth is projected to be greatest. Mango (*Mangifera indica* L.) represents one of the most widely produced and traded tropical fruits with production globally in excess of 57 Mt in 2021 (FAOSTAT 2023). In Australia, mango production was ~64 Kt in 2023/24 with a market value of greater than AUD$220 million (Hort Innovation 2024).

In temperate tree fruit crops (e.g., apples and pears), modern orchard management, including the adoption of dwarf cultivars, modified tree architecture and high-density planting has contributed to substantial yield and resource-efficiency gains (Tustin et al. 2022). Similar work to intensify production in tropical fruit systems, such as mango, has included the application of genetic techniques to identify prospective cultivars (Wilkinson et al. 2022), use of high-efficiency irrigation/fertigation technologies such as sensor-mediated Regulated Deficit Irrigation (Vélez-Sánchez et al. 2021) and canopy manipulation (i.e., pruning and espalier training) (Menzel and Le Lagadec 2017, Ibell et al. 2024). Traditionally, mango orchards were established at low tree densities (i.e., 100–200 trees ha^{-1}) with individual trees eventually attaining heights and widths of up to 10 m, with a dense and self-shading canopy architecture. It is believed that the development of novel high-density orchard systems (Dickinson and Bennett 2021) including modified canopies will improve light interception and canopy light-use efficiency by optimizing the light interception by individual leaves leading to enhanced orchard performance (Willaume et al. 2004, Kishore et al. 2023, Mahmud et al. 2023). At the same time, protected cropping systems for mango have been implemented to avoid excess temperatures and associated fruit sunburn (Jutamanee and Onnom 2016, Scuderi et al. 2022). Understanding how changes in canopy structure and shading will affect tree performance are critical to the assessment of these techniques moving forward.

Gradients in light quantity and quality are one of the defining features of mature tree canopies (Niinemets et al. 2015) with leaf-level photosynthetic attributes and related leaf functional traits acclimating to these gradients (Meir et al. 2002). Specifically, leaves receiving more incident light, by being higher in the canopy, often exhibit increased maximum photosynthetic assimilation per unit leaf area, a higher leaf mass per unit area (LMA), a higher nitrogen content per unit area, and in some cases, a larger proportion of photosynthetic nitrogen in components critical for photosynthesis (Niinemets et al. 2015, Niinemets 2023). However, the associations between leaf functional traits and the distribution of nitrogen across plant canopies may vary according to species and are often found to be 'sub-optimal' from models that consider whole-canopy nitrogen efficiency (Meir et al. 2002, Buckley et al. 2013). Explanations for the apparent suboptimal nitrogen distribution include high costs for nitrogen reallocation when light availability changes, the issue of leaf-age profiles changing through plant canopies (Niinemets 2016), or a constraint emerging from species specific LMA (Dewar et al. 2012). As such, within-canopy light acclimation responses are still poorly understood and this complicates inclusion of within canopy trait variations in both canopy (van der Meer et al. 2023) and landscape scale photosynthesis models (Rogers et al. 2017).

Under well-managed orchard conditions (i.e., no nutrient or water limitation) whole-plant primary productivity should be determined by spatial and temporal gradients of light present within the canopy and the capacity of leaf-level function to acclimate to these gradients (Rosati and Dejong 2003, Carrié et al. 2023). While tree pruning and training systems, such as espalier or palmette, that seek to maximize individual leaf light-exposure may maximize productivity, there exists a light spectral and intensity range for optimal leaf photosynthesis (Schaffer and Gaye 1989, Johnson 1998). Above a saturation level, individual leaves may be unable to use additional incident light with resulting high temperatures and the generation of oxidative stress leading to photoinhibition and a reduction in photosynthesis (Johnson 1998, Weng et al. 2013, Jutamanee and Onnom 2016). In addition, to counter the generation of reactive oxygen species in sun-exposed leaves, biosynthesis of antioxidant capacity such as phenolic compounds may be upregulated, potentially reducing net primary productivity (Linatoc et al. 2018).

Determining integrated responses to novel orchard management requires either prolonged and expensive field trials; or the development of spatially explicit structural-functional models. These models, such as Y-plant (Pearcy and Yang 1996) or broader frameworks such as Helios (Bailey 2019) seek to replicate canopies as three-dimensional structures that must perform multiple simultaneous tasks—and which may result in less-than-optimal behaviour with respect to a single process, such as light capture (Pearcy et al. 2005). Canopies used in these modelling efforts can be based upon either pure theoretical representations (Génard et al. 2000) or observed canopies captured using LiDAR scanning (Bailey 2019, Dian et al. 2023). However, in all cases, understanding how leaf-level function and trait plasticity in target species and cultivars responds to environmental conditions such as light is a pre-requisite in such modelling efforts, allowing us to develop our understanding of how novel-orchard management may impact whole-canopy function and productivity into the future.

In this study, we quantified leaf-level functional response to a gradient in light intensity within a highly productive, dwarf mango cultivar. Specifically, we examined (i) how foliar biochemical, morphological and physiological traits are distributed in relation to light availability across conventional tree canopies and (ii) how changes to canopy structure through espalier training may alter individual leaf-level light interception and functional traits leading to a change in canopy-scale productivity. In doing so, we aimed to provide insight into how canopy manipulation may impact leaf function and thereby whole-canopy responses.

Materials and methods

Study area and experimental sampling

Leaf samples from across a range of light environments were collected over 4 days at the Walkamin Research Station of the Queensland Department of Primary Industries, Mango Planting System Experiment (17° 8′ 17″ S, 145° 25′ 41″ E; elevation 599 m) previously described in Ibell et al. (2024) and Sun et al. (2021). The site has a 10-year mean daily minimum and maximum temperature of 17.2 ± 3.3 °C and 28.1 ± 3.5 °C,

respectively, with a distinct dry/cool, wet/hot tropical climate (Figure S1 available as Supplementary Data at *Tree Physiology* Online, Australian Bureau of Meteorology station ID 31108). To enable sampling from across a complete range in sunlight exposure, while accounting for the known influence of leaf age on leaf function (Niinemets 2016), samples were taken from a single-age cohort of leaves (current year's flush) across three trees of the mango variety Calypso™, planted at 416 trees ha^{-1} with a wide, open-vase (conventional) canopy (Figure S2 available as Supplementary Data at *Tree Physiology* Online). The Calypso™ cultivar currently accounts for ~25% of Australian mango production (Wilkinson et al. 2022), has expanding international production and is a good candidate for intensive canopy manipulation (Mahmud et al. 2019, 2023).

After characterization of the leaf-specific light environment (see section Determining light environment), data on leaf-level gas exchange were collected in situ (details below) using a portable photosynthesis analyser (LI-6400XT, LiCOR Biosciences, Lincoln, NE, USA). Subsequently, leaves were detached, weighed for fresh weight, measured for lamina thickness (microtome), scanned (Cannon LiDEe 400) to determine individual leaf area, and analysed for chlorophyll content and light transmission/reflectance (details below). Fresh leaves were then wrapped in aluminium foil and snap frozen in liquid nitrogen (~20 min after harvest) and held at −80 °C until lyophilization. Dried samples were then reweighed to determine dry leaf mass and ground (Rocklabs Bench Top Ring Mill) to a fine powder before determination of basic biochemical characteristics including total carbon and nitrogen, $\delta^{13}C$ and total phenolic content (TPC).

Determining light environment

Prior to leaf sampling, light meters (HOBO MX220 lux meters, HOBO Data Loggers Australia) were affixed to the branch apical growing tip. Light meters were held in place using zip ties and orientated to match the plane of the target leaves. Data were recorded at 5 min intervals and converted from Lux to photosynthetic photon flux density (PPFD, $\mu mol\ m^{-2}\ s^{-1}$) using a standard ratio for sunlight (i.e., 0.0185, https://www.apogeeinstruments.com/conversion-ppfd-to-lux/). Data for 11 days prior to leaf harvest (7 July 2022 to 18 July 2022) were used to characterize the light environment of each sampled leaf and compared with two meters held in a horizontal plane in a nearby unobstructed field.

Leaf-level gas exchange

Two portable photosynthesis analysers (LI-6400xt, Li-Cor Biosciences, Lincoln, IL, USA) fitted with CO_2 mixer (6400-01 CO_2 Mixer) and LED light source (6400-02B light source) were used to collect in situ gas exchange data on a subset of 52 leaves of the 68 sampled for morphological and biochemical analysis. An initial estimate of light-saturated photosynthesis (A_{sat}) was collected on each leaf (410 p.p.m. CO_2, 1500 $\mu mol\ m^{-2}\ s^{-1}$ PPFD) which was used to estimate the maximum velocity of carboxylation (V_{cmax}) using the 'one-point method' (De Kauwe et al. 2016) with curve fitting without an assumption of triose phosphate use limitation utilizing the *plantecophys* R-package (Duursma 2015). Subsequently, the response of photosynthesis (A_{net}) to PPFD for each leaf was determined over a 13-point light-response curve (PPFD equal to 2500, 2000, 1500, 1000, 750, 500, 200, 120, 70, 40, 20, 10, 0). Fitting of a non-rectangular hyperbolic model to the observed light response data (Marshall and Biscoe 1980) was carried out for each leaf using the function R package *photosynthesis* (Stinziano et al. 2023) allowing the determination of four fitting parameters; light saturated photosynthesis (A_{sat}), dark respiration (R_d), α (photochemical efficiency of photosynthesis at low light) and θ (ratio of physical to total resistance to diffusion of CO_2). This also allowed for the determination of the light compensation point (LCP), the light intensity at which there is no net exchange of CO_2.

Light reflectance/transmission/absorption

Fresh leaves were initially assessed for chlorophyl content using a standard chlorophyll concentration meter (MC100-Apogee) before reflectance (R) and transmittance (T) spectra from all wavelengths between 390 and 1100 nm were collected for the adaxial side of leaves using a UV/Visible spectrometer (Ocean Optics Jaz UV/Visible Spectrophotometer, Cole-Parmer, Vernon Hills, IL, USA) and external type integrating sphere (LI-1800-12, LI-COR Biosciences, Lincoln, USA) with a quartz-halogen light source (LiCOR Biosciences). Settings within the Ocean optics software included scan averaging equal to 40, and a boxcar width equal to 5, with a nonlinearity correction and initial reference made to a barium sulphate standard. Each leaf had a reflectance sample, reflectance reference, transmittance reference and a transmittance sample taken. A dark reference was collected every 10–15 min. Leaf absorptance (A) was then calculated from R and T, (corrected for leaf-scan reference) using the equation $A = 1 - R - T$. A tripod was used to keep the orientation of the integrating sphere stable for all measurements. The average transmission/reflectance of all shortwave radiation (PAR, i.e., 400–1000 nm) was used for canopy light environment modelling (see below). Whilst specific wavelengths were used to calculate the photochemical reflectance index (PRI) as an estimate of light-use efficiency, specifically reflectance at 531 nm (a waveband sensitive to the xanthophyl cycle) and 570 nm as a reference using Eq. (1).

$$PRI = \frac{(R_{531} - R_{570})}{(R_{531} + R_{570})} \quad (1)$$

Using this definition, a positive PRI value indicates high light-use efficiency, while negative or lower PRI values are indicative of reduced light-use efficiency (Peñuelas et al. 1995).

Biochemical characterization of leaves

Total elemental and isotopic composition

The carbon and nitrogen content (%C and %N) and stable isotope ratio ($\delta^{13}C$) in dried and ground leaf material was determined using a Costech Elemental Analyser fitted with a zero-blank auto-sampler coupled via a ConFloIV to a ThermoFinnigan DeltaVPLUS using Continuous-Flow Isotope Ratio Mass Spectrometry (EA-IRMS) at Washington State University Stable Isotope Core Laboratory. Stable isotope results are reported as per mil (‰) deviations from the Vienna Pee Dee Belemnite (VPDB) standard ($\delta^{13}C$) after a two-point normalization and corrections for drift and sample size. Carbon isotope fractionation $\Delta^{13}C$ was calculated from $\delta^{13}C$ according to the equation of Farquhar et al. (1989) and assuming a constant $\delta^{13}C$ of atmospheric CO_2 of −8‰.

Leaf-level estimates of the unified stomatal optimization term g_1 (Medlyn et al. 2011) were made from the $\Delta^{13}C$ values using Eq. (2).

$$g_1 = \frac{\left(\frac{C_i}{C_a}\sqrt{VPD}\right)}{\left(1 - \frac{C_i}{C_a}\right)} \quad (2)$$

VPD is the average daytime vapour pressure deficit (VPD; assumed here to be 1 kPa) and $\frac{C_i}{C_a}$ is estimated from Eq. (3).

$$\frac{C_i}{C_a} = \frac{\left(\Delta^{13}C - a'\right)}{\left(b' - a'\right)} \quad (3)$$

In Eq. (3), a' is the isotope fractionation arising from diffusion through the stomata and b' the net fractionation caused by carboxylation, with standard values for C_3 plants of 4.4‰ and 27‰, respectively (Bloomfield et al. 2019).

Total phenolic content

Powdered leaf samples (~30 mg) were extracted in cold 50% acetone with TPC measured by the Folin–Ciocalteu method as modified by Ritmejerytė et al. (2019). Briefly, a 20-μL aliquot of the leaf extract and 380 μL distilled H_2O were mixed with 25 μL Folin–Ciocalteu reagent. After 3 min, 75 μL 20% Na_2CO_3 (w/v) was added to the reaction mixture and incubated in the assay tubes at room temperature for 20 min. The absorbance of the mixture was then measured at 765 nm with a microplate reader (FLUOstar OPTIMA, BMG LABTECH Pty Ltd). Gallic acid was used as a standard and TPC was expressed as Gallic acid equivalents (mg GAE g^{-1} dry weight).

Canopy modelling

Digital representations of mango tree canopies coupled to ray tracing was used to examine the likely light interception by individual leaves within canopy architectures. To create the digital trees, a structural model of branching architecture was created based on a LiDAR point cloud of real trees before the recreation of the leaf canopy positions via a mathematical representation of observed leafing patterns.

In January 2022, a terrestrial LiDAR scanner (Riegl AZ-400i, Riegl Laser Measurement Systems, Horn, Austria) was used to scan a conventional open-vase canopy mango tree from six separate locations equidistant around the tree. The same LiDAR scanner was then mounted on a buggy vehicle to scan an espalier-trained tree from both sides. The raw point cloud dataset was exported and registered using RiScan Pro. V2 (Riegl Laser Measurement Systems) and processed further with CloudCompare (https://www.danielgm.net/cc/) to extract branching architecture features—including the 3D coordinates of branch start and end points, as well as branch diameters. These extracted features were then used to inform a C++ programme for structural reconstruction. Leaf propagation across the LiDAR developed tree structure was based on functional-structural plant modelling parameterized for *Mangifera indica* cv. Calypso by Mizani (2019). Specifically, on all branches between 10 and 40 leaves were randomly propagated along each branch segment at an average insertion angle of 61° to the branch axis. Leaf size was randomly assigned, with length ranging from 110 to 259 mm, and leaf width from 40 to 65 mm.

An initial ray-tracing simulation was run for individual digital trees using a Central Processing Unit based high-performance light simulator (University of Queensland; unpublished). The generation of rays from the sky was based on Cieslak et al. (2008) using Quasi-Monte Carlo simulation and CIE (Commission Internationale de l'Eclairage) standard clear sky model (CIE-110, 1994) while the tracing of explicit rays (including reflection, transmission and absorption) was deployed across multiple CPU cores (deployable on either a single or multiple compute nodes) for parallel implementation within a single simulation task. For this study, each light tracing run used 32 million explicit rays from the sky, with the latitude and longitude set at −17.13 °N and 145.43 °E and date set to July 9 (Julian day 190).

As the observations of leaf position by Mizani (2019) were taken from young canopies and were applied here across mature canopy branching structure it was found to erroneously assign an excess number of leaves to older portions of the canopy when compared with previously published literature (Yu et al. 2016, Boudon et al. 2020), resulting in a distribution of light within the canopies that did not reflect previous assessments of light distribution within the canopy of these specific experimental orchards (Westling et al. 2020). As a result, after an initial simulation all propagated leaves with energy values < 1.4% of incident light were 'digitally pruned' (removed) and the light model was rerun to determine distribution of light intensity across realistic digital canopies. The level used for digital pruning was based upon the lowest recorded leaf-specific light environment in our captured dataset (see Data availability statement) and the extremely low probability of mango leaf survival at light levels below this (Boudon et al. 2020).

Data analysis

All analyses and graphical representations were performed using R version 4.2.2. The light environment of sampled leaves was characterized by taking the average daytime (06:30–18:30 h) and maximum, defined here as 95th percentile light intensity, observed at each leaf location for the 11 days prior to sampling. To determine if the average light conditions experienced by a leaf significantly impacted upon its morphological and biochemical characteristics, we applied a simple linear model (estimated using OLS) between the target parameters and average daily PPFD. An initial analysis that included tree identity as a random factor showed no significant differences between the three trees used and so was dropped for presented analyses.

Total leaf-level net-assimilation (A_{total}, mmol m^{-2} day^{-1}) averaged for the 11 days preceding leaf sampling was modelled using the *PhotosynEB* function from the *plantecophys* V1.4-6 R-package (Duursma 2015). Leaf specific morphological (i.e., absorbance, leaf width) and physiological (i.e., V_{cmax}, J_{max}, θ, g_1, R_d) characteristics were coupled with the observed time course of illumination at each leaf, assuming a Medlyn et al. (2011) model of stomatal optimization. Meteorological conditions, including air temperature, windspeed and VPD, were assumed to be uniform across all leaves but varied over time based on data from the experimental site meteorology station (Davis Vantage Pro2). Since PhotosynEB models leaf temperature as a function of leaf traits and meteorological conditions, leaf temperature will vary across leaves despite the uniform meteorological inputs.

Once A_{total} was calculated for each leaf, we examined the trend with increasing average PPFD ($PPFD_{av}$) using both a linear response and saturating response curve based upon Michaelis–Menten kinetics fitted in R using *nls* (Eq. (4). Model fits were compared on the basis of both calculated R^2 and Akaike Information Criterion (AIC).

$$A_{total} = \frac{A_{(total,\ \max)} \times PPFD_{av}}{K_m + PPFD_{av}} \quad (4)$$

Subsequently, we calculated instantaneous photosynthetic nitrogen-use efficiency (PNUE, μmol g^{-1} s^{-1}) as light-saturated photosynthetic rate (A_{sat}, μmol m^{-2} s^{-1}) divided by leaf total nitrogen content on an areal basis (N_A, g m^{-2}) and leaf-level net-assimilation nitrogen-use efficiency (A_{total}—NUE, mmol g^{-1} day^{-1}) using predicted A_{total} (mmol m^{-2} day^{-1}) divided by nitrogen content (N_A g m^{-2}).

Light interception of leaves within digital tree canopies was normalized to the maximum level observed via monitoring. To this distribution we applied the Michaelis–Menten function fitted above to predict changes in whole-canopy total assimilation.

Results

Light environment

The light environment experienced by leaves sampled from mature mango canopies was complex and highly variable (Figure 1), ranging from internal canopy leaves that received no or only brief periods of direct illumination, to those at the canopy's outer fringes, which—due to their orientation and exposure—experienced high levels of illumination for >6h per day. There was a distinctly non-linear relationship between average daytime irradiance (μmol m^{-2} s^{-1}) or total daily irradiance (mol m^{-2} day^{-1}), and maximum irradiance (μmol m^{-2} s^{-1})—expressed as 95th percentile. This positive bias towards higher daytime maximum values shows the large number of leaves in which the total incoming irradiance was dominated by short-duration high-intensity sunflecks.

Foliar morphological and biochemical traits

Across sampled leaves, we observed a strong relationship between leaf width and individual leaf area (β = 28 ± 1.0 cm^2 cm^{-1}, $F_{(1,66)}$ = 447.5, P < 0.001, R^2 = 0.94). However, there was no trend seen in individual leaf area with increasing irradiance ($F_{(1,66)}$ = 3.5, P = 0.066, R^2 = 0.05, Figure S3A available as Supplementary Data at *Tree Physiology* Online). We did find that both LMA ($F_{(1,66)}$ = 94.9, P < 0.001, R^2 = 0.59) and leaf dry matter content (LDMC) ($F_{(1,66)}$ = 58.47, P < 0.001, R^2 = 0.47) increased with higher irradiance, with LMA and LDMC rising on average 57 g m^{-2} and 70 mg g^{-1}, respectively, over the range of irradiance seen in mature Calypso canopies (Figure S3B and Cavailable as Supplementary Data at *Tree Physiology* Online). Carbon isotope discrimination ($\Delta^{13}C$) ranged from 20.8 to 24.5‰ averaging 22.6 ± 0.8‰, with a significant decline ($F_{(1,66)}$ = 31.3, P < 0.001, R^2 = 0.31) with increasing irradiance. Due to the covarying nature of both LMA and $\Delta^{13}C$ across light environment we found a strong negative correlation between $\Delta^{13}C$ and LMA ($F_{(1,66)}$ = 49.5, P < 0.001, R^2 = 0.43).

Chlorophyll concentration on an areal basis (Chl_A) showed no significant trend with either average irradiance or maximum irradiance, averaging 383 ± 61 μmol m^{-2} (345 ± 54 mg m^{-2}) across all leaves tested (Figure 2A). However, when expressed on a mass-basis chlorophyl content (Chl_M) averaged 2.7 ± 0.6 mg g^{-1} and showed a significant ($F_{(1,66)}$ = 88.4, P < 0.001, R^2 = 0.57) decline with increasing irradiance (Figure 2B). In contrast, both nitrogen content on an areal (N_A) basis ($F_{(1,66)}$ = 78.8, P < 0.001, R^2 = 0.50, Figure 2C) and a mass (N_M) basis ($F_{(1,66)}$ = 19.6, P < 0.001, R^2 = 0.23, Figure 2D) showed a highly significant increase in leaves under higher irradiance. Combined, these relationships also resulted in a highly significant ($F_{(1,66)}$ = 115.7, P < 0.001, R^2 = 0.64, Figure 2E) decline in the ratio of chlorophyl to leaf total nitrogen content ranging from 0.25 in the most shaded leaves to 0.13 in leaves exposed to the highest irradiance. Assuming a constant nitrogen content of chlorophyll as the average for both Chlorophyll a and b (i.e., 6.23%) this meant that the amount of leaf total nitrogen present as chlorophyll

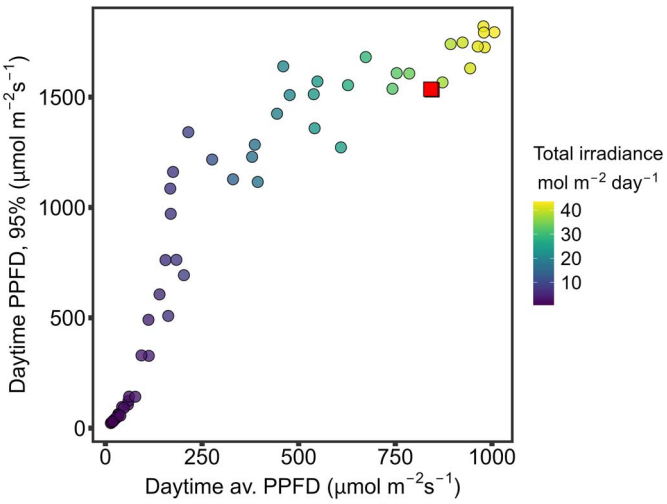

Figure 1. Characterization of light environment of 68 leaves sampled from the canopies of mango (*Mangifera indica* cv. Calypso) trees with a wide, open vase-canopy typical of Australian production. Light characterization carried out for 11 days prior to leaf-sampling examining daytime (i.e., 06:30–18:30 h) average PPFD, daytime maximum light level experienced (i.e., 95%) and total irradiance (Mol m^{-2} day^{-1}) accumulated over this monitoring period. Square symbols represent replicate conditions measured parallel to the ground surface in a nearby clearing.

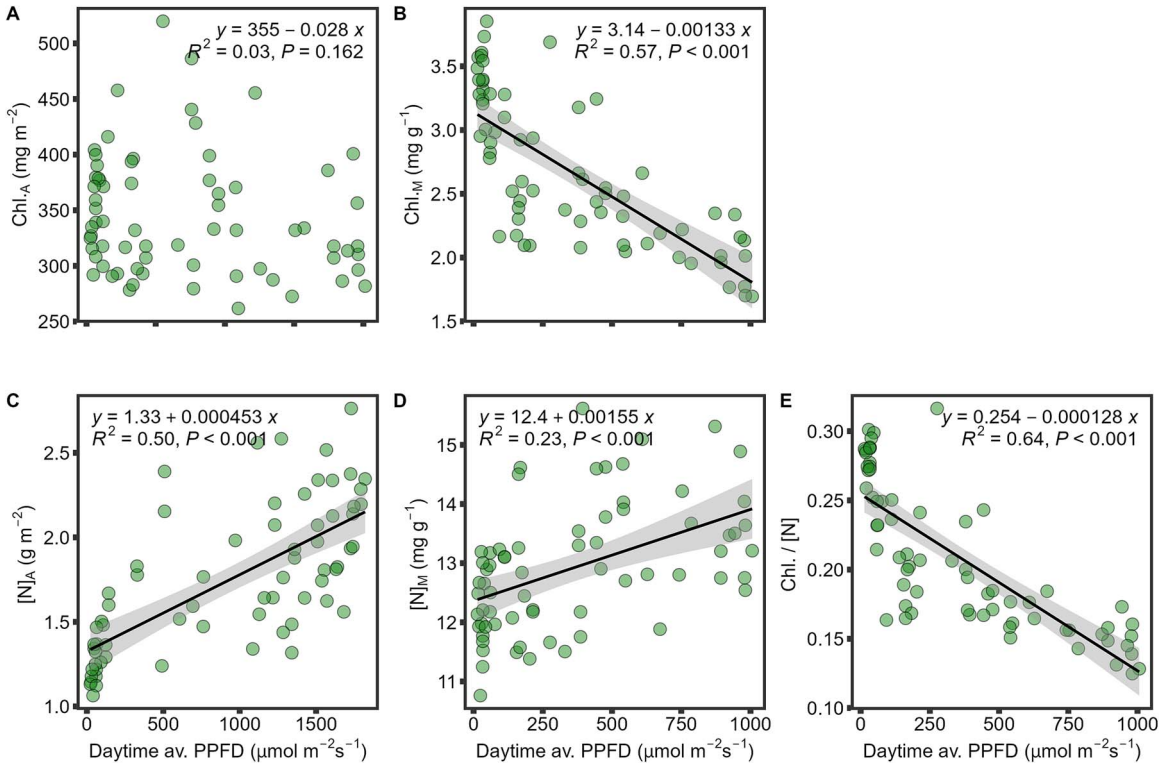

Figure 2. Chlorophyll (A, B), total nitrogen (C, D) content, expressed on an areal basis (A, C) and a leaf dry mass basis (B, D) basis—and the ratio of chlorophyll to total nitrogen concentration (E) in a single-aged cohort of leaves of mango sampled from across a gradient in light exposure experienced in a mature tree canopy.

declined from 1.6 to 0.78% across the range of canopy irradiance tested.

Leaf level transmission and reflectance of shortwave radiation (i.e., 400 to 1000 nm) varied over the range of wavelengths observed (Figure S4 available as Supplementary Data at *Tree Physiology* Online), however, leaf level transmission as a proportion of all wavelengths between 400 and 1000 nm averaged 0.22 ± 0.015 across all leaves, and was found to decline in leaves developed under higher irradiance ($F_{(1, 66)}$ = 30.8, P < 0 0.001, R^2 = 0.32, Figure S5A available as Supplementary Data at *Tree Physiology* Online), while average reflectance was found to significantly increase ($F_{(1, 66)}$ = 43.02, P < 0.001, R^2 = 0.39, Figure S5C available as Supplementary Data at *Tree Physiology* Online). Due to the noted variation in LMA across irradiance both transmission ($F_{(1, 66)}$ = 156.6, P < 0.001, R^2 = 0.70, Figure S5B available as Supplementary Data at *Tree Physiology* Online) and reflectance ($F_{(1, 66)}$ = 44.8, P < 0.001, R^2 = 0.40 Figure S5D available as Supplementary Data at *Tree Physiology* Online) were shown to have significant and opposite relationships with LMA (Figure S5B and D available as Supplementary Data at *Tree Physiology* Online).

The PRI metric, an estimate of light-use efficiency, showed a significant decline from fully shaded to exposed leaves ($F_{(1, 66)}$ = 134.0, P < 0.001, R^2 = 0.67, Figure 3A). TPC on a mass basis averaged 46 ± 6.2 mg_{GAE} g^{-1} across all leaves and showed a subtle but highly significant ($F_{(1, 66)}$ = 11.5, P = 0.001, R^2 = 0.15) increase with increasing irradiance (Figure 3B). Furthermore, when expressed on an areal basis (Figure 3C) the additional impact of observed trend in LMA resulted in a highly significant ($F_{(1, 66)}$ = 66.8, P < 0.001, R^2 = 0.50, Figure 3C) and substantial increase across irradiance with TPC (g_{GAE} m^{-2}) increasing by >70% across the range of irradiance sampled.

Foliar physiological traits

In those leaves in which gas exchange data were collected (n = 52), V_{cmax} ($F_{(1, 50)}$ = 15.3, P < 0.001, R^2 = 0.23), A_{sat} ($F_{(1, 50)}$ = 12.5, P < 0.001, R^2 = 0.20, Figure 4A) and LCP ($F_{(1, 50)}$ = 91.5, P < 0.001, R^2 = 0.65, Figure 4B) for photosynthesis all increased with increasing average leaf-level daytime irradiance.

Leaf-level total productivity (A_{total}) significantly increased with increasing irradiance across the tree canopy (Figure 4C) when modelled for individual leaves using observed light response characteristics, modelled leaf temperature and measured light environment for each leaf. Fitting a simple linear model demonstrated the rise to be statistically significant ($F_{(1,50)}$ = 97.5, P < 0.001, R^2 = 0.66). However, a saturating Michaelis–Menten function resulted in a better fit to the modelled data when considering either R^2 (i.e., 0.70) or AIC (Figure 4C). A saturating function is also more physiologically appropriate for extreme high and low light levels. Fitting of this saturating function yielded an $A_{total\text{-}max}$ of 199 ± 33 mmol m^{-2} day^{-1} and K constant of 439 ± 160.

When PNUE was calculated as A_{sat}/N_A there was no significant trend ($F_{(50,1)}$ = 0.05, P = 0.83) with light availability, averaging 3.7 ± 1.1 μmol g^{-1} s^{-1} in all leaves (Figure S6A available as Supplementary Data at *Tree Physiology* Online). However, when we considered A_{total}-NUE, we saw that average PPFD explained a statistically significant and moderate proportion of the variance observed ($F_{(50,1)}$ = 49.3, P = 0.002, R^2 = 0.50). Moreover, as with A_{total}, we found

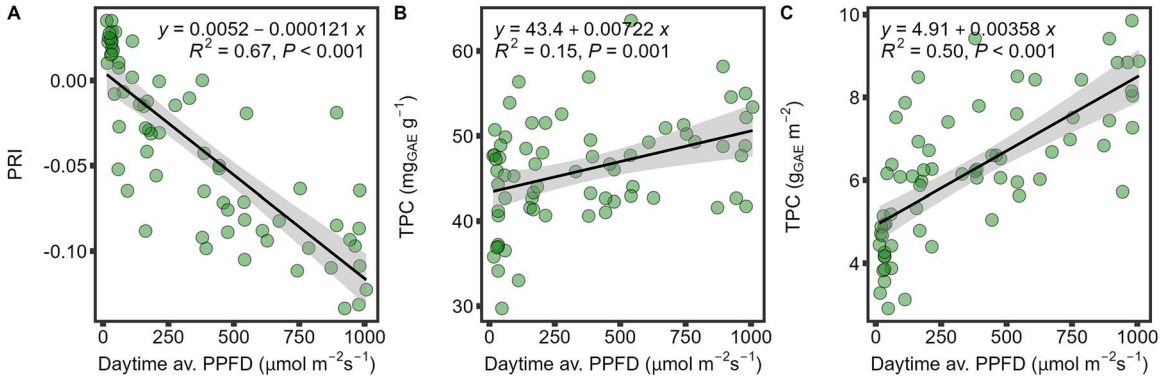

Figure 3. Photochemical reflectance index (PRI) (A) and total phenolic content (TPC) expressed as a mass (B) or area (C) of leaf tissue in a single-aged cohort of leaves of mango sampled from across a gradient in light exposure experienced in a mature tree canopy.

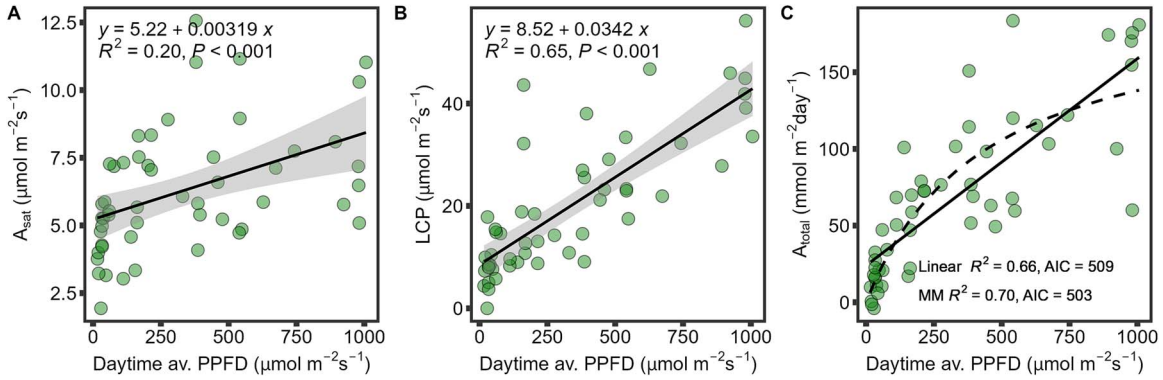

Figure 4. Light saturated photosynthesis (A_{sat}, A) and light compensation point (LCP, B) across a light gradient determined by leaf-level gas exchange in 52 mango leaves, in addition to modelled leaf-level total net assimilation (A_{total}) of leaves for the 11 days prior to sampling (C).

that a saturating Michaelis–Menten function resulted in a better fit to the data when considering either R^2 (i.e., 0.59) or AIC (Figure S6B available as Supplementary Data at *Tree Physiology* Online). Fitting of this saturating function yielded a maximum A_{total}-NUE of 74.8 ± 8.8 mmol g^{-1} day^{-1} and K constant of 176 ± 63.

Comparison of canopy architecture

Digital representation of canopy architecture under wide conventional and narrow espalier-trellis training were used to examine the likely difference in sunlight distribution in mango tree canopies (Figure 5). Comparison of the digital canopies showed that leaves under both architectures were highly heterogeneous and showed right-skewed distributions of relative sunlight interception, with skewness values (D'Agostino test) of 1.46 and 1.24 in conventional and espalier-trellis canopies, respectively. This suggests that while most leaves in both canopies receive much lower levels of sunlight than the most exposed leaves, the leaves in the espalier-trellis canopy were slightly more evenly spread. With leaf area weighted means of relative energy interception in the narrow espalier-trellis canopy being 0.311 ± 0.146 (mean ± 1 SD) as compared with 0.296 ± 0.154 in the wide conventional canopy.

When we applied the Michaelis–Menten function relating relative sunlight interception to leaf-level total net-assimilation (i.e., $A_{total\text{-}max}$ of 199 ± 33 mmol m^{-2} day^{-1} and K constant of 0.436 ± 0.0.159) to predict the influence of altered canopy architecture on total canopy productivity we saw that total canopy productivity was 6.5% greater in the tree with the conventional canopy as compared with the espalier-trellis canopy—due to the 9.0% decrease in total canopy leaf area (i.e., 26.8 vs 24.4 m^2). When standardized for total canopy leaf area, on the other hand, we found that the espalier-trellis canopy actually had a 3.6% increase in whole-canopy productivity over the conventional canopy architecture as a result of having a greater proportion of leaves more highly illuminated.

Discussion

This study examined how leaves of mango (*Mangifera indica* cv. Calypso) show acclimation in physiological, biochemical and morphological traits in response to light intensity gradients found within mature tree canopies. Our findings provide valuable insights into how light-driven trait plasticity and canopy structure influence leaf- and thereby canopy-level function, informing strategies for orchard management and productivity optimization in mango cultivation.

Light environment and leaf-level acclimation

The gradients of light availability within the mango canopy highlighted the heterogeneity of light interception by leaves, consistent with findings in other tree species (Niinemets et al. 2015). The distinct skewness in light distribution reinforces the challenge of achieving an optimal canopy structure through natural development, particularly in dense canopies where shaded leaves contribute disproportionately less to whole-canopy productivity (Rosati and Dejong 2003). The non-linear relationship between average and maximum PPFD suggests that sunflecks define the light environment across

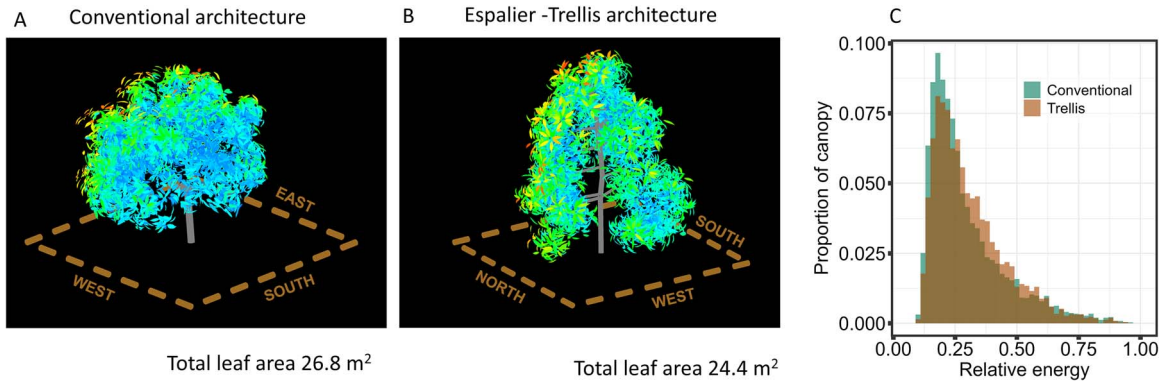

Figure 5. Digital representation of mango tree canopies under (A) conventional (wide, open-vase) and (B) narrow espalier-trellis architecture, with ray tracing for a single day 2022-07-09 used to simulate leaf-level light interception—colour heat ramp indicates the relative summed illumination. The distribution of relative leaf area found across illumination also provided in subplot (C).

much of the mid and even upper canopy, a feature common in many tree canopies (Durand et al. 2022).

Leaf-level traits showed clear acclimation to light gradients, with increases in LMA, LDMC and nitrogen content on an area basis under higher light availability. We also observed a 61% increase in light saturated photosynthetic capacity (A_{sat}) and 395% increase in light compensation point (LCP) across the range in leaf irradiance observed. These changes align with well-documented acclimation responses, where sun-exposed leaves exhibit higher structural investment and photosynthetic capacity to maximize light use (Niinemets 2023). The observed decline in $\Delta^{13}C$ with increasing irradiance may also reflect this changing photosynthetic capacity throughout the canopy. However, there is also the potential for increasing mesophyll CO_2 diffusion resistance with increasing LMA (Vitousek et al. 1990) and modified CO_2 source signature to play a role (Cheesman et al. 2020).

Biochemical trade-offs and light use efficiency

Increasing light exposure resulted in a decline in chlorophyll content per unit mass (Chl_M) and chlorophyll-to-nitrogen ratio (Figure 2). This reflects a shift in resource allocation towards traits that support structural and biochemical resilience rather than light capture alone. Similar trends have been reported in other species, where nitrogen is increasingly allocated to other components of the photosynthetic machinery under high light (Buckley et al. 2013). The increase in TPC in sun-exposed leaves suggests a photoprotective strategy (Schneider et al. 2019), mitigating oxidative stress from high irradiance and associated reactive oxygen species (Linatoc et al. 2018). This biochemical investment, while beneficial for photoprotection, may incur a trade-off with whole leaf lifespan net carbon gain. This is supported by previous findings where the use of shade cloth to mitigate excess solar radiation in mango actually saw an increase in fruit yield (Jutamanee and Onnom 2016, Shaban et al. 2021).

The PRI was found to decline with increasing light exposure, indicative of lower light-use efficiency in sunlit leaves. This suggests that despite higher photosynthetic capacity, light-saturated leaves may operate less efficiently, particularly under supra-optimal light conditions that induce photoinhibition (Johnson 1998). Such findings highlight the importance of balancing light interception and photoprotection in canopy management strategies and obtaining optimal, rather than maximal, light environments.

Productivity and canopy-level implications

Modelled leaf-level total net-assimilation (A_{total}) for the 11 days prior to sampling increased significantly with light availability, following a saturating response curve (Figure 4C). This aligns with the assumption that sun-exposed leaves were generally more productive than those deeper in the canopy. However, it is also clear that productivity saturates at high light intensities due to limitations in biochemical capacity, and increasing non-photochemical processes, as indicated by increased phenolic content and decreased PRI. The diminishing returns of increasing light exposure of leaves already at high light levels emphasizes the need to focus on efficient light distribution across the whole-canopy if canopy-scale productivity is to be increased.

Digital canopy modelling demonstrated that in a narrow, espalier-trellis trained system, compared with a wide, open-vase canopy system, light interception per unit leaf area was slightly increased but total canopy net assimilation was lower due to a 9% reduction in canopy leaf area. However, when standardized for total canopy leaf area, the espalier-trellis canopy actually exhibited a modest increase in productivity. These findings, similar to those of Kishore et al. (2023), suggest that espalier-trellis systems may offer advantages in terms of light distribution and resource-use efficiency, all else being equal. This could be particularly relevant to high-density orchard systems, as it should be noted that the conventional open-vase trees used here had a footprint of 8 × 6 m as compared with a narrow espalier-trellis tree's footprint of just 4 × 2 m (i.e., 1/6 of the space). It should also be noted that the LiDAR scanning used to capture tree canopy architecture in this study was conducted at a single point in time pre-fruit-set. During the year the shape of a conventional mango tree canopy varies substantially due to the impact of increasing fruit-load, and associated branch bending. As such, repeated scans throughout the year, and extended modelling of productivity over the entire year, would be needed to capture the full effect of modified canopy architecture on whole-canopy productivity. Moving forward it would also be important to expand the ray tracing and light modelling framework to account for changing light quality found throughout the canopy (Carrié et al. 2023).

Increased canopy-level productivity does not necessarily translate into greater fruit yield due to the complexity of intra-canopy resource allocation across spatial and temporal scales (Génard et al. 2008, Auzmendi and Hanan 2020). However,

mechanistic canopy models that incorporate LiDAR-derived digital tree representations offer a valuable means to assess how changes in leaf-level function and canopy architecture influence both tree-level (Jung et al. 2018) and orchard-scale carbon capture (Dian et al. 2023). These models enable the integration of spatially explicit light dynamics with leaf-level physiology, which when coupled to models of carbon allocation to fruits (Génard et al. 2008) offer a pathway for refining orchard design and management practices. Future work should therefore explore the interaction between modified canopy structure, environmental stressors such as elevated temperatures, and whole-tree fruit production, particularly under scenarios of increasing climate extremes.

Acknowledgments

We would like to thank Zac Scobell for field-work support and Dr Nara Oliveira Vogado for laboratory assistance in the determination of leaf phenolic content. The authors also thank Riegl Australia for providing access to their LiDAR scanner and analysis software.

Supplementary Data

Supplementary data for this article are available at *Tree Physiology* Online.

Author contributions

A.W.C., R.O. and L.A.C. designed and conceived of the study. Data were collected by A.W.C., K.B.M., L.H. and G.R. Data analysis was led by A.W.C. with inputs from K.B.M. and L.H., and interpretation from all authors. A.W.C. wrote the manuscript with inputs from all authors.

Conflict of interest

The authors declare no conflicts of interest.

Funding

Support for this work came from Queensland Department of Primary Industries via the National Tree Crop Intensification in Horticulture Program (AS18000) funded through Hort Innovation Frontiers. The LiDAR data collection and processing was funded through the Queensland Reef Water Quality Program—Digital Horticulture project by the Queensland Department of Primary Industries.

Data availability

All leaf-level functional trait and meteorological data used in this article are available at Dryad, DOI: https://doi.org/10.5061/dryad.v41ns1s6k.

References

Auzmendi I, Hanan JS (2020) Investigating tree and fruit growth through functional-structural modelling: implications of carbon autonomy at different scales. Ann Bot 126:775–788. https://doi.org/10.1093/aob/mcaa098.

Bailey BN (2019) Helios: a scalable 3D plant and environmental biophysical modeling framework. Front Plant Sci 10:1185. https://doi.org/10.3389/fpls.2019.01185.

Bloomfield KJ, Prentice IC, Cernusak LA et al. (2019) The validity of optimal leaf traits modelled on environmental conditions. New Phytol 221:1409–1423. https://doi.org/10.1111/nph.15495.

Boudon F, Persello S, Grechi I, Marquier A, Soria C, Fournier C, Léchaudel M, Normand F (2020) Assessing the role of ageing and light availability in leaf mortality in the mango tree. International Society for Horticultural Science (ISHS), Leuven, Belgium, pp 601–608.

Buckley TN, Cescatti A, Farquhar GD (2013) What does optimization theory actually predict about crown profiles of photosynthetic capacity when models incorporate greater realism? Plant Cell Environ 36:1547–1563. https://doi.org/10.1111/pce.12091.

Carrié E, Grechi I, Boudon F, Frak E, Combes D, Normand F (2023) Modeling functional relationships between morphogenetically active radiation and photosynthetic photon flux density in mango tree crown. Front Ecol Evol 11:17. https://doi.org/10.3389/fevo.2023.1046332.

Cheesman AW, Duff H, Hill K, Cernusak LA, McInerney FA (2020) Isotopic and morphologic proxies for reconstructing light environment and leaf function of fossil leaves: a modern calibration in the Daintree Rainforest, Australia. Am J Bot 107:1165–1176. https://doi.org/10.1002/ajb2.1523.

Cieslak M, Lemieux C, Hanan J, Prusinkiewicz P (2008) Quasi-Monte Carlo simulation of the light environment of plants. Funct Plant Biol 35:837–849. https://doi.org/10.1071/FP08082.

De Kauwe MG, Lin YS, Wright IJ et al. (2016) A test of the 'one-point method' for estimating maximum carboxylation capacity from field-measured, light-saturated photosynthesis. New Phytol 210:1130–1144. https://doi.org/10.1111/nph.13815.

Dewar RC, Tarvainen L, Parker K, Wallin G, McMurtrie RE (2012) Why does leaf nitrogen decline within tree canopies less rapidly than light? An explanation from optimization subject to a lower bound on leaf mass per area. Tree Physiol 32:520–534. https://doi.org/10.1093/treephys/tps044.

Dian Y, Liu X, Hu L et al. (2023) Characteristics of photosynthesis and vertical canopy architecture of citrus trees under two labor-saving cultivation modes using unmanned aerial vehicle (UAV)-based LiDAR data in citrus orchards. Hortic Res 10:uhad018. https://doi.org/10.1093/hr/uhad018.

Dickinson G, Bennett D (2021) Establishment of high-density mango orchards. Cooperative Research Centre for Developing Northern Australia, Townsville, p 25.

Durand M, Stangl ZR, Salmon Y, Burgess AJ, Murchie EH, Robson TM (2022) Sunflecks in the upper canopy: dynamics of light-use efficiency in sun and shade leaves of *Fagus sylvatica*. New Phytol 235:1365–1378. https://doi.org/10.1111/nph.18222.

Duursma RA (2015) Plantecophys—an R package for analysing and modelling leaf gas exchange data. PloS One 10:13. https://doi.org/10.1371/journal.pone.0143346.

FAOSTAT (2023) Statistical database. Food and Agriculture Organization of the United Nations, Rome.

Farquhar GD, Ehleringer JR, Hubick KT (1989) Carbon isotope discrimination and photosynthesis. Annu Rev Plant Physiol Plant Mol Biol 40:503–537. https://doi.org/10.1146/annurev.pp.40.060189.002443.

Génard M, Baret F, Simon D (2000) A 3D peach canopy model used to evaluate the effect of tree architecture and density on photosynthesis at a range of scales. Ecol Model 128:197–209. https://doi.org/10.1016/S0304-3800(99)00232-X.

Génard M, Dauzat J, Franck N, Lescourret F, Moitrier N, Vaast P, Vercambre G (2008) Carbon allocation in fruit trees: from theory to modelling. Trees Struct Funct 22:269–282. https://doi.org/10.1007/s00468-007-0176-5.

Hort Innovation (2024) All fruit - overview. In: Australian horticulture statistics handbook 2023/24. Horticulture Innovation Australia Limited, Sydney, pp 29–181.

Ibell PT, Normand F, Wright CL, Mahmud K, Bally ISE (2024) The effects of planting density, training system and cultivar on vegetative growth and fruit production in young mango (*Mangifera indica* L.) trees. Horticulturae 10:23.

Johnson PR (1998) Leaf gas exchange as influenced by environmental factors in mango cultivars (*Mangifera indica* L.), grown in the semi arid tropics, PhD thesis. Adelaide University.

Jung DH, Lee JW, Kang WH, Hwang IH, Son JE (2018) Estimation of whole plant photosynthetic rate of Irwin mango under artificial and natural lights using a three-dimensional plant model and ray-tracing. Int J Mol Sci 19:152. https://doi.org/10.3390/ijms19010152.

Jutamanee K, Onnom S (2016) Improving photosynthetic performance and some fruit quality traits in mango trees by shading. Photosynthetica 54:542–550. https://doi.org/10.1007/s11099-016-0210-1.

Kishore K, Singh HS, Nath V, Baig MJ, Murthy DS, Acharya GC, Behera S (2023) Influence of canopy architecture on photosynthetic parameters and fruit quality of mango in tropical region of India. Hortic Environ Biotechnol 64:557–569. https://doi.org/10.1007/s13580-022-00500-z.

Linatoc A, Idris A, Abu Bakar MF (2018) Influence of light intensity on the photosynthesis and phenolic contents of *Mangifera Indica*. J Sci Technol 10:47–54. https://doi.org/10.30880/jst.2018.10.04.009.

Mahmud K, Ibell P, Wright C, Scobell Z, Wilkie J, Bally I (2019) Light relation in intensive mango orchards. Proceedings 36:122.

Mahmud KP, Ibell PT, Wright CL, Monks D, Bally I (2023) High-density espalier trained mangoes make better use of light. Agronomy 13:14. https://doi.org/10.3390/agronomy13102557.

Marshall B, Biscoe PV (1980) A model for C3 leaves describing the dependence of net photosynthesis on irradiance. 2. Application to the analysis of flay leaf photosynthesis. J Exp Bot 31:41–48. https://doi.org/10.1093/jxb/31.1.41.

Medlyn BE, Duursma RA, Eamus D et al. (2011) Reconciling the optimal and empirical approaches to modelling stomatal conductance. Glob Chang Biol 17:2134–2144. https://doi.org/10.1111/j.1365-2486.2010.02375.x.

van der Meer M, Lee H, de Visser PHB, Heuvelink E, Marcelis LFM (2023) Consequences of interplant trait variation for canopy light absorption and photosynthesis. Front Plant Sci 14:1012718. https://doi.org/10.3389/fpls.2023.1012718.

Meir P, Kruijt B, Broadmeadow M, Barbosa E, Kull O, Carswell F, Nobre A, Jarvis PG (2002) Acclimation of photosynthetic capacity to irradiance in tree canopies in relation to leaf nitrogen concentration and leaf mass per unit area. Plant Cell Environ 25:343–357. https://doi.org/10.1046/j.0016-8025.2001.00811.x.

Menzel CM, Le Lagadec MD (2017) Can the productivity of mango orchards be increased by using high-density plantings? Sci Hortic 219:222–263. https://doi.org/10.1016/j.scienta.2016.11.041.

Mizani A (2019) Managing vigour, light, crop load and tree architecture in mango to maximise productivity and quality. PhD thesis, The University of Queensland.

Niinemets Ü (2016) Leaf age dependent changes in within-canopy variation in leaf functional traits: a meta-analysis. J Plant Res 129:313–338. https://doi.org/10.1007/s10265-016-0815-2.

Niinemets U (2023) Variation in leaf photosynthetic capacity within plant canopies: optimization, structural, and physiological constraints and inefficiencies. Photosynth Res 158:131–149. https://doi.org/10.1007/s11120-023-01043-9.

Niinemets Ü, Keenan TF, Hallik L (2015) A worldwide analysis of within-canopy variations in leaf structural, chemical and physiological traits across plant functional types. New Phytol 205:973–993. https://doi.org/10.1111/nph.13096.

Pearcy RW, Yang WM (1996) A three-dimensional crown architecture model for assessment of light capture and carbon gain by understory plants. Oecologia 108:1–12. https://doi.org/10.1007/BF00333208.

Pearcy RW, Muraoka H, Valladares F (2005) Crown architecture in sun and shade environments: assessing function and trade-offs with a three-dimensional simulation model. New Phytol 166:791–800. https://doi.org/10.1111/j.1469-8137.2005.01328.x.

Peñuelas J, Filella I, Gamon JA (1995) Assessment of photosynthetic radiation-use efficiency with spectral reflectance. New Phytol 131:291–296. https://doi.org/10.1111/j.1469-8137.1995.tb03064.x.

Ritmejerytė E, Boughton BA, Bayly MJ, Miller RE (2019) Divergent responses of above- and below-ground chemical defence to nitrogen and phosphorus supply in waratahs (*Telopea speciosissima*). Funct Plant Biol 46:1134–1145. https://doi.org/10.1071/FP19122.

Rogers A, Medlyn BE, Dukes JS et al. (2017) A roadmap for improving the representation of photosynthesis in earth system models. New Phytol 213:22–42. https://doi.org/10.1111/nph.14283.

Rosati A, Dejong TM (2003) Estimating photosynthetic radiation use efficiency using incident light and photosynthesis of individual leaves. Ann Bot 91:869–877. https://doi.org/10.1093/aob/mcg094.

Schaffer B, Gaye G (1989) Gas exchange, chlorophyll and nitrogen content of mango leaves as influenced by light environment. HortScience 24:507–509. https://doi.org/10.21273/HORTSCI.24.3.507.

Schneider GF, Coley PD, Younkin GC, Forrister DL, Mills AG, Kursar TA (2019) Phenolics lie at the centre of functional versatility in the responses of two phytochemically diverse tropical trees to canopy thinning. J Exp Bot 70:5853–5864. https://doi.org/10.1093/jxb/erz308.

Scuderi D, Gugliuzza G, Di Salvo G, Priola F, Passafiume R, Farina V (2022) Shading net and partial covering plastic film do not affect phenology, photosynthetic activity or fruit quality traits of Kensington pride mango. Plants 11:16.

Shaban AEA, Rashedy AA, El-Banna MIM (2021) Mitigation of excessive solar radiation and water stress on 'Keitt' mango *Mangifera indica* trees through shading. Acta Sci Pol Hortorum Cultus 20:77–88. https://doi.org/10.24326/asphc.2021.4.7.

Stinziano JR, Roback C, Gamble D, Murphy B, Hudson P, Muir CD (2023) R package - photosynthesis: tools for plant ecophysiology & modeling, R package version 2.1.4.

Sun WL, Xu ZH, Ibell P, Bally I (2021) Genetic and environmental influence on foliar carbon isotope composition, nitrogen availability and fruit yield of 5-year-old mango plantation in tropical Australia. J Soil Sediment 21:1609–1620. https://doi.org/10.1007/s11368-020-02850-6.

Tustin DS, Breen KC, van Hooijdonk BM (2022) Light utilisation, leaf canopy properties and fruiting responses of narrow-row, planar cordon apple orchard planting systems-a study of the productivity of apple. Sci Hortic 294:110778. https://doi.org/10.1016/j.scienta.2021.110778.

Vélez-Sánchez JE, Balaguera-López HE, Alvarez-Herrera JG (2021) Effect of regulated deficit irrigation (RDI) on the production and quality of pear Triunfo de Viena variety under tropical conditions. Sci Hortic 278:109880. https://doi.org/10.1016/j.scienta.2020.109880.

Vitousek PM, Field CB, Matson PA (1990) Variation in foliar $\delta^{13}C$ in Hawaiian *Metrosideros polymorpha*: a case of internal resistance? Oecologia 84:362–370. https://doi.org/10.1007/BF00329760.

Weng J-H, Wong S-L, Lin R-J, Jhaung L-H (2013) Quantitative effects of temperature and light intensity on PSII efficiency of mango leaves under artificial and natural conditions. J For Res 18:371–378. https://doi.org/10.1007/s10310-012-0359-9.

Westling F, Mahmud K, Underwood J, Bally I (2020) Replacing traditional light measurement with LiDAR based methods in orchards. Comput Electron Agr 179:105798. https://doi.org/10.1016/j.compag.2020.105798.

Wilkinson MJ, Yamashita R, James ME, Bally ISE, Dillon NL, Ali A, Hardner CM, Ortiz-Barrientos D (2022) The influence of genetic structure on phenotypic diversity in the Australian mango (*Mangifera indica*) gene pool. Sci Rep 12:20614. https://doi.org/10.1038/s41598-022-24800-7.

Willaume M, Lauri P-É, Sinoquet H (2004) Light interception in apple trees influenced by canopy architecture manipulation. Trees 18:705–713. https://doi.org/10.1007/s00468-004-0357-4.

Yu X, White N, Lisle A, Cao SF, Zhang Y, Joyce DC, Hofman PJ. (2016) 3D modelling of mango fruit skin blush in the tree canopy. In: Drew R, Fitch M, Zhu J (eds), 29th International Horticultural Congress on Horticulture - Sustaining Lives, Livelihoods and Landscapes (IHC)/4th International Symposium on Papaya/8th International Pineapple Symposium/International Symposium on Mango. International Society for Horticultural Science, Brisbane, Australia, pp 341–345.

Tree Physiology, 2025, 45, tpaf109
https://doi.org/10.1093/treephys/tpaf109
Research paper